Thin Solid Films, *218* (1992) 304–309

Basic elements for photodeposited high T_c thin film devices

J. Flokstra, R. P. J. IJsselsteijn and J. W. M. Hilgenkamp

Department of Applied Physics, University of Twente, P.O. Box 217, 7500 AE Enschede (The Netherlands)

(Received December 8, 1991; accepted January 7, 1992)

Abstract

Flat films, high quality insulating layers and adequately superconducting via contacts are basic elements for high T_c device fabrication. We studied the influence of the process parameters of laser deposition on the occurrence of droplets and outgrowths in YBaCuO films. The droplet density is minimal when a laser fluence below about 1.0 J cm^{-2} is used. The outgrowth density decreases with increasing laser pulse rate or decreasing deposition temperature. High quality flat films were obtained with a rate of 10 Hz and at a temperature of 720 °C. Wet chemical etching and etching with an Argon ion source were used for structuring multilayers with $SrTiO_3$ as an insulating layer. Smooth edges were obtained with an argon gun. Bromine and EDTA etching are not adequate techniques for fabricating controllable well-defined edges. Cross-overs, via contacts and coils were prepared.

1. Introduction

Among the preparation methods for high T_c thin films, the photodeposition technique based on pulsed UV lasers has obtained a special position. The fast deposition rate and the conservation of compound stoichiometry has led to an extended use of this relatively new and simple thin film preparation method. Numerous groups have shown that high quality films can be easily fabricated [1].

During the last few years high T_c thin film research has shifted towards the development of active devices like junctions and superconducting quantum interference devices (SQUIDs). Various types of junctions have been prepared as grain boundary junctions, step edge and edge junctions, normal metal bridge junctions and multilayer structures. Laser ablation has also proved to be a valuable technique [2].

It is well known from devices based on classical superconductors that the number of levels in a multilayer structure increases with the complexity of the device. In a d.c. SQUID, for instance, external signals are coupled to the SQUID hole using a planar input coil integrated on top of the SQUID washer [3]. The insulation between current carrying layers then has to be of high quality to prevent unwanted short circuits. Necessary contacts through insulating layers should be such that the superconducting contact is strong and no weak link is formed leading to undesirable perturbing effects in the electrical properties of the device.

From the above it is clear that flat layers, high quality insulating layers and good via contacts are basic elements in high T_c device fabrication. This paper describes our research on these subjects.

The laser ablation technique introduces microstructural irregularities in and on the film. In the next section we present a study on the deposited material distribution and the droplet and outgrowth formation of $YBa_2Cu_3O_7$ films as a function of the process conditions. Optimal settings of the process parameters for flat film production are then derived.

The structuring of layers of $YBa_2Cu_3O_7$ and multilayers including $SrTiO_3$ as an insulator are then discussed and the results of wet chemical and ion beam etching described. The fabrication of smooth edges is very important for high T_c structures as cross-overs and coils. The properties of via contacts are also discussed.

Two types of junctions and SQUIDs are studied in our laboratory, grain boundary junctions on bi-crystals and on templates, and edge junctions [4]. A bi-crystal junction is an example of a one-layer device. The smoothness of a film plays also an important role for this device, especially the growth at the artificial grain boundary. We will see that the initial film growth leads to many small particles on substrate scratches and this may also be expected on the artificial grain boundary, leading to uncontrollable junction characteristics. Multilayer structures are necessary for template and edge junctions. Film smoothness and the structure of the edges is in this case of utmost importance. The edge junctions have a base and insulating layer prepared by sputtering or by laser ablation and a top layer deposited by sputtering. Results on such junctions have been published in ref. 4.

0040-6090/92/$5.00

2. Thin films prepared by laser ablation

Laser-deposited films generally contain droplets and outgrowths [5, 6]. When the laser beam hits the target, the YBaCuO melts in a few nanoseconds and the evaporated material strongly interacts with the incoming pulse. This leads to a very hot and dense plasma just in front of the target. Immediately after the pulse an adiabatic expansion of this hot gas takes place in all directions. It is most likely that the shock wave produces droplet-like particles (dimensions of the order of 1–2 μm) when it hits the target that reach the substrate after a more or less ballistic transport. During the thin film growth at standard deposition temperatures the $YBa_2Cu_3O_7$ forms a c-axis oriented film; small particles (dimensions up to 0.1–0.2 μm) with a-axis orientation may also grow leading to regions peaking out of the film surface due to the higher growth rate in that direction [7].

The number of droplets and outgrowths per unit film area can be influenced by the deposition parameters. We used an LPX 110 CC excimer laser in the XeCl mode ($\lambda = 308$ nm, $\tau = 20$ ns). The bundle was focused on a rotating YBaCuO target placed inside a vacuum chamber. Oxygen pressure (standard 25 Pa) and distance between target and substrate (standard 35 mm) are always chosen so that the film is formed at the edge of the plasma.

The droplet density was studied using silicon wafers of 5 cm at ambient temperature as a substrate. The sticking of the material in the amorphous YBaCuO layer will be complete so that a reliable picture of the droplet formation relative to the atomic YBaCuO formation can be obtained. It is clear that the droplet density has to be normalized with respect to layer thickness. As well as counting the droplets the layer thickness also has to be determined.

We varied the laser pulse energy between 58 and 98 mJ, having a beam spot size at the target of 0.8 mm^2 and 2.5 mm^2. In a third series a constant laser energy of 90 mJ was used varying the spot size between 0.8 and 7.3 mm^2. In the case of the 0.8 mm^2 spot size the plasma has a spherical shape leading to a cylindrical material distribution. The plasma is conically shaped for larger spot sizes resulting in an ellipsoidal geometry of the film thickness.

The maximum thickness d of the deposited layer (1200 pulses) is found to be, in good approximation [5]: (i) proportional to the spot size S at constant laser energy E; (ii) proportional to E at constant S. Thus d is proportional to $S \cdot E$ or, when the laser fluence Φ_e is used, to $\Phi_e S^2$. A closer look at the low energy density dependence of the layer thickness shows a threshold value in the material distribution of 0.4 J cm^{-2}, so that

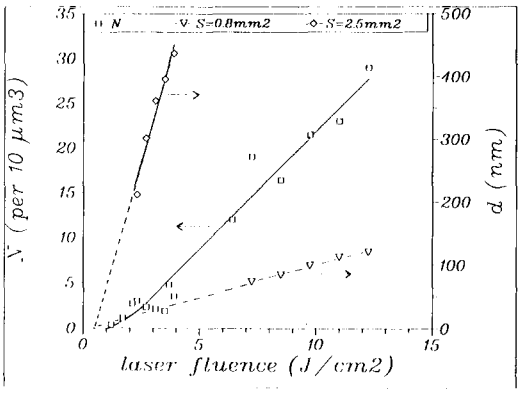

Fig. 1. The droplet density on an area of 100 μm^2 normalized for a layer thickness of 100 nm, and the layer thickness as a function of the laser beam energy density.

$$d \propto (\Phi_e - 0.4) \cdot S^2$$

The droplet density normalized with respect to the thickness, $\bar{N}$, is in good approximation [5]: (i) proportional to E at constant S; (ii) proportional to $1/S$ at constant E, so that $\bar{N} \propto E/S$ or $\bar{N} \propto \Phi_e$. In this case a threshold energy of about 1.0 J cm^{-2} is found so that

$$\bar{N} \propto (\Phi_e - 1.0)$$

The combination of these two results gives the number of droplets per unit area, N, as

$$N \propto (\Phi_e - 0.4)(\Phi_e - 1.0) \cdot S^2 \cdot n_s$$

with n_s the number of pulses and $\Phi_e > 1.0$ J cm^{-2}. In Fig. 1 the layer thickness and the number of droplets on an area of 100 μm^2 of a 100 nm thick layer are given as function of the laser fluence. It is clear that layers with a minimum number of droplets should be prepared at a laser fluence of about 1 J cm^{-2}. At this energy density the laser ablation process is already rather effective but the plasma in front of the target does not become hot enough to remove the droplets from the target. The number of droplets for a standard layer of 100 nm is less than 1 on an area of 200 μm^2.

We also studied the droplet density as a function of the target density. Home-made targets with densities between 80% and 94% of the theoretical density were used, but we did not observe a clear influence on the droplet density. A 100% density target from industry turned out to be of 93% density and resulted in droplet densities similar to these of our own high density targets.

The occurrence of outgrowths has been studied for YBaCuO layers on $SrTiO_3$ and YSZ substrates [5]. The laser fluence was taken as 1.2 J cm^{-2} and the spot size as 7.3 mm^2 so that the films are almost droplet free. We varied the number of pulses, the laser pulse frequency and the temperature of the substrate.

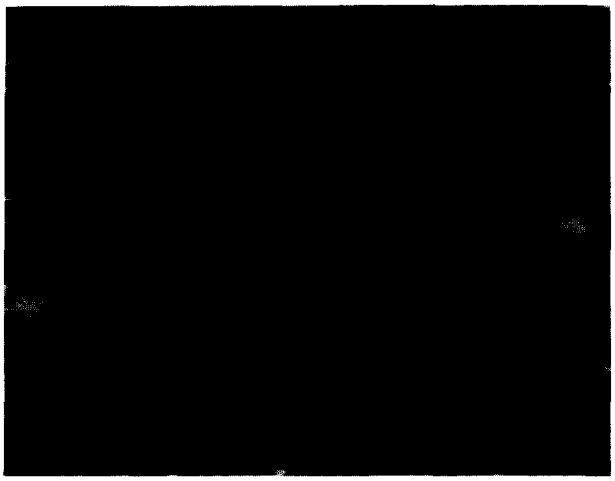

(a)

(b)

Fig. 2. SEM pictures of $YBa_2Cu_3O_7$ films on $SrTiO_3$ substrates. The film shown in (a) is about 15 nm thick and contains many small particles. The preference for substrate scratches can be seen. The film shown in (b) is about 100 nm thick and shows the larger outgrowths. (The bar is 1 μm.)

Thin layers (15 nm) exhibit a large amount of small particulates more or less concentrated on scratches in the substrate (Fig. 2). When the thickness increases a much smaller number of particles remain, whereas the particle dimensions have increased to about 0.1–0.2 μm. These particles are most probably *a*-axis oriented $YBa_2Cu_3O_7$ outgrowths [7].

The outgrowth density gradually decreases when the pulse frequency is increased. A layer 100 nm thick prepared at a substrate temperature of 770 °C contains about 50 outgrowths per 100 μm^2 at a pulse frequency of 0.2 Hz and 0.4 outgrowths at 100 Hz. The onset and zero resistivity temperature are somewhat lowered at this high rate, most probably due to a lack of oxygen near the substrate during the layer formation.

The outgrowth density also decreases when the substrate temperature is lowered. At 720 °C the density is below 1 per 100 μm^2 for a pulse rate of 2 Hz. The superconducting properties of the film have not deteriorated, as is the case at the deposition temperature of 700 °C. Optimal preparation conditions are thus a pulse rate of 10 Hz and a deposition temperature of 720 °C.

In spite of these optimalization studies for the fabrication of flat films, it still remains difficult to produce large areas without severe defects. This severely hampers the development of devices consisting of many layers on top of each other.

3. Structuring layers and multilayers

As mentioned in the introduction, the fabrication of high-quality insulating layers and via contacts are necessary keystones in device fabrication. The insulating layer on top of a structured base layer is not a flat film, but it follows the structure of the layer underneath. Especially at the edges this may lead to severe problems and fabrication of smooth edges is therefore of top priority. Our research concerns the fabrication of crossing superconducting striplines and via contacts being the ingredients for a high T_c input coil for a d.c. SQUID.

The material for the insulating layer has to be non-reactive with $YBa_2Cu_3O_7$ and oxygen-permeable. The deposition temperature has to be comparable to that of YBaCuO. Furthermore the crystallographic fit with YBaCuO has to be good and the thermal expansion coefficients should not differ too much. Although several materials can be used we have chosen $SrTiO_3$ because the deposition conditions of this material are quite similar to those of YBaCuO [8] and the interdiffusion is negligible.

We prepared bi-layers of $SrTiO_3$ on top of $YBa_2Cu_3O_7$. The base layer was deposited using the optimal conditions mentioned previously. The $SrTiO_3$ layer was prepared at substrate temperatures of about 730 °C, an oxygen pressure of 15 Pa and a laser pulse energy density of 1.4 J cm^{-2}. X-ray diffraction measurements on these bi-layers on a (100) oriented yttrium-stabilized ZrO_2 substrate only show (001) reflections of the $SrTiO_3$. No other phases are found.

If we examine the smoothness of the $SrTiO_3$ layers on top of the YBaCuO thin film, large differences can be seen to be caused by only small changes in deposition temperature. The difference of the deposition temperatures for a closed smooth surface and for a surface with holes or outgrowths is only 10 °C. The surface of the YBaCuO bottom layer plays an important role if several layers are deposited on top of each other. SEM pictures show a decreasing surface smoothness for each next layer in a YBaCuO–$SrTiO_3$–YBaCuO tri-layer.

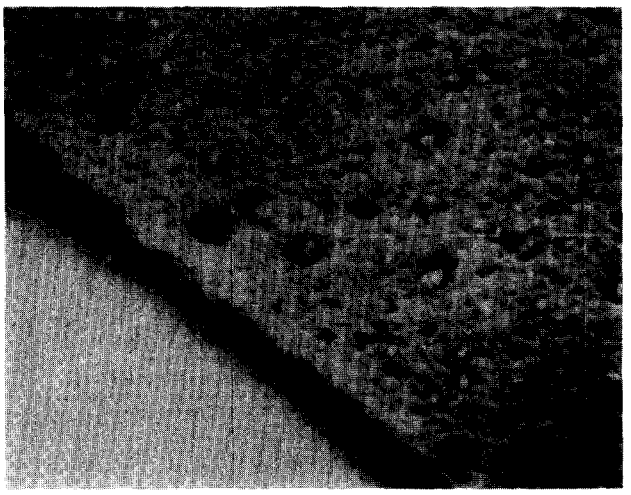

Fig. 3. SEM picture showing the result of a 250 nm thick $YBa_2Cu_3O_7$ film after etching with a bromine solution.

In order to grow $SrTiO_3$ and $YBa_2Cu_3O_7$ epitaxially on top of the edge of a $YBa_2Cu_3O_7$ stripline, the edge should be very smooth and have an angle of 30° or less with the substrate surface [9]. For this reason etching methods which yield steep edges, like etching with diluted H_3PO_4 or argon ion etching, are not suitable. To produce low angles we etched in three different ways. We investigated etching in a 2% solution of Br in ethanol [10], wet chemical etching in a solution of EDTA in water [11], and etching with an Ar ion-gun. For all three methods standard photolithography is used to define the structure which is to be etched away.

For the experiments with the 2% Br solution the $YBa_2Cu_3O_7$ layers were first etched with a diluted H_3PO_4 solution (1:150). After the removal of the photoresist, the $YBa_2Cu_3O_7$ layers were etched with the Br solution to smoothen the edges. A scanning electron micrograph (SEM) picture of a YBCO layer etched for 60 s in a 2% Br solution is shown in Fig. 3. It can be seen that this method does not decrease the steepness of the edges but does degrade the surface smoothness of the YBCO film.

The etching with EDTA was carried out with a solution of 37 g $Na_2 \cdot EDTA \cdot 2H_2O + 4.0$ g NaOH in 1000 ml water and a saturated solution of EDTA as reported in the literature [11]. Etching of a YBCO film 100 nm thick, partly covered with standard photoresist took 1000 s yielding severe underetching, resulting in a not very well defined edge with holes in it. The saturated EDTA solution yielded smoother edges. However, these edges were not very well defined.

For the etching with the Ar ion-gun, a photoresist layer was baked out in an oven at 90 °C for 10 min. After structuring the photoresist, the sample was placed in a vacuum chamber having a background pressure of 10^{-4} Pa. An Ar ion-gun was positioned at about 10 cm from the substrate. The angle between the substrate normal and the Ar ions was 45°.

The pulsed structuring took place using an Ar pressure of 5×10^{-2} Pa, resulting in an effective etch rate of 40 nm min^{-1}. SEM pictures of the resulting edges are shown in Fig. 4. In both pictures the Ar ions were coming from the left side. It can clearly be seen that both edges of the photoresist layer can be etched in the same etch run.

If we use photoresist which is more hardened, caused by increased baking or an increased period between baking of the photoresist and the etching, only one

(a)

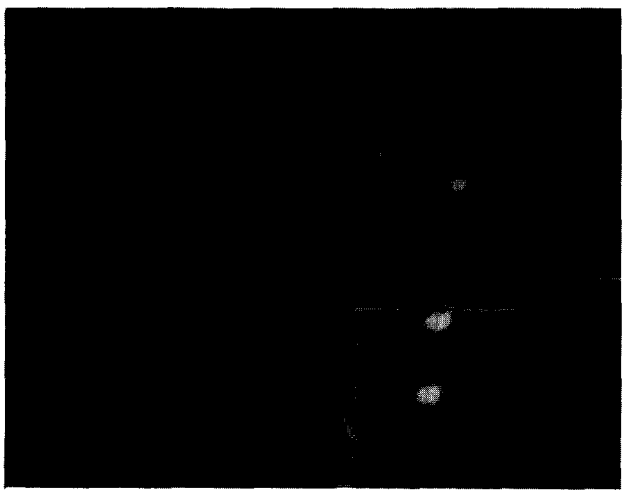

(b)

Fig. 4. Smooth edges of a 300 nm thick $YBa_2Cu_3O_7$ layer produced by one Ar ion beam etch run. The Ar beam came from the left side at an angle of 45°.

smooth edge is obtained. The edge facing the Ar ions does not become smooth.

Using the Ar ion-gun etching procedure cross-overs, window contacts and multiturn coils have been fabricated. The base $YBa_2Cu_3O_7$ layer of the cross-over has a thickness of 200 nm and is etched into a stripline of 150 μm width using the ion beam. On top of the $YBa_2Cu_3O_7$ layer a (100) oriented $SrTiO_3$ layer of 150 nm is grown. The 200 nm thick $YBa_2Cu_3O_7$ top layer is structured into a 30 μm wide and 1000 μm long stripline using Ar ion etching. The critical temperature of the $YBa_2Cu_3O_7$ top layer is 87 K. At 4.2 K, J_c equalled 5×10^5 A cm^{-2}. The resistivity of the $SrTiO_3$ layer at 77 K was 6×10^5 Ω cm.

The base $YBa_2Cu_3O_7$ layer (thickness 200 nm) for the window contact is structured using the Ar ion-gun before a 150 nm thick $SrTiO_3$ overlayer is deposited. A window of 60×60 μm is etched in this overlayer using the Ar ion-gun. The $YBa_2Cu_3O_7$ top electrode (200 nm) is structured using Ar ion etching. The critical temperature of the window contact is 84 K. The critical current density is 9×10^2 A cm^{-2} at 77 K. This value can be improved by making the contact in such a way that the current path lies in the a–b plane.

A high T_c superconducting coil has been made based on the fabrication process for the cross-overs and window contact as described above. The base $YBa_2Cu_3O_7$ layer was 300 nm thick and structured into a 150 μm wide stripline with two smooth edges using the Ar ion-gun. This stripline serves as a contact from the inner part of the multiturn coil. The second layer consists of a 100 nm thick $SrTiO_3$ layer. A window of 60×60 μm^2 is etched with the Ar gun down into the $YBa_2Cu_3O_7$ layer. After cleaning the film surfaces by Ar ion milling (removal of about 4 nm), the top $YBa_2Cu_3O_7$ (200 nm) layer has been deposited and structured into a multiturn coil by Ar ion etching. A SEM picture of the multiturn coil is given in Fig. 5. Four point measurements yielded a critical temperature of 27 K and a critical current density of 4×10^2 A cm^{-2} at 4.2 K. After the coil had been broken in the centre by wet chemical etching, it was no longer superconducting, proving that no short circuits are present between the base and top $YBa_2Cu_3O_7$ layers. Improvements on the coil are in progress.

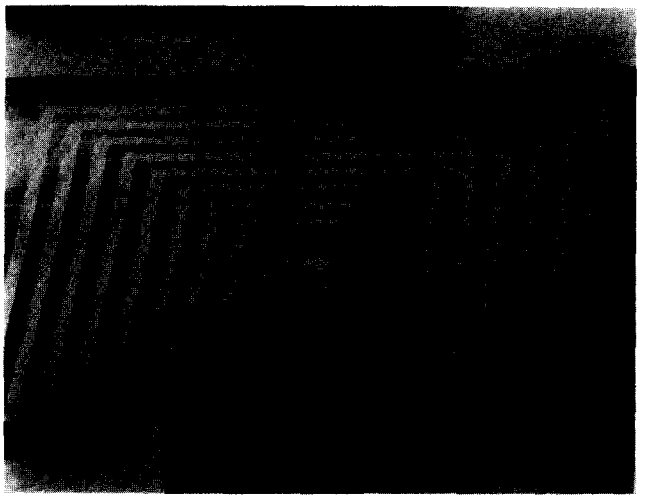

Fig. 5. SEM picture of an 8 turn high T_c coil made from $YBa_2Cu_3O_7$ and $SrTiO_3$ as an insulating layer.

4. Discussion and conclusions

The process conditions for obtaining $YBa_2Cu_3O_7$ films with a minimum number of droplets and outgrowths using the laser deposition technique have been described. When the laser fluence is below about 0.4 J cm^{-2} no material transport takes place. It can be calculated that the YBaCuO material simply does not reach the melting temperature [5]. Droplets are formed when the laser fluence exceeds the value of about 1.0 J cm^{-2}. The droplets come from the target when the adiabatic expansion of hot plasma takes place just in front of the target.

The formation of outgrowths is a general problem in thin film deposition techniques. We found that the density of outgrowths could be reduced by increasing the pulse rate of the laser ablation or by decreasing the substrate temperature during the deposition.

Smooth edges are necessary to prevent electrical short circuits between superconducting layers separated by an insulating layer. Wet chemical etching turned out not to be a suitable technique. Well-defined edges can be obtained with an Argon ion-gun. It was possible to fabricate cross-overs and via contacts as well as high T_c coils.

The development of methods for fabrication of the basic elements for high T_c devices is of crucial importance for junction and SQUID fabrication.

Acknowledgments

The authors are greatly indebted to D. H. A. Blank and H. Rogalla for their involvement in this research, and to F. Bartolomé Usieto and A. J. H. M. Rijnders for the technical assistance.

References

1 D. C. Paine and J. C. Bravman (eds.), *Laser Ablation for Materials Synthesis*, Vol. 191, Materials Research Society, 1990.

2 G. Koren, E. Aharoni, E. Polturak and D. Cohen, *Appl. Phys. Lett.*, *58* (1990) 634.
K. Char, M. S. Colclough, S. M. Garrison, N. Newman and G. Zaharchuk, *Appl. Phys Lett.*, *59* (1991) 733.
R. Gross and P. Chaudhari, in A. Barone (ed.), *Principles and Applications of Superconducting Quantum Interference Devices*, World Scientific, Singapore, 1991.
3 J. M. Jaycox and M. B. Ketchen, *IEEE Trans. Magn.*, *17* (1990) 400.
4 J. Gao, Y. Boguslavskii, B. B. G. Klopman, D. Terpstra, G. J. Gerritsma and H. Rogalla, *Appl. Phys Lett.*, *59* (1991) 2754.
5 D. H. A. Blank, R. P. J. IJsselsteijn, P. G. Out, H. J. H. Kuiper, J. Flokstra and H. Rogalla, *Mat. Sci. Eng. B*, *13* (1992) 67.
6 R. P. J. IJsselsteijn, D. H. A. Blank, P. G. Out, F. J. G. Roesthuis, J. Flokstra and H. Rogalla, *Proc. E-MRS Strasbourg*, (1991) 251.
7 R. Ramesh, A. Inam, D. M. Hwang, T. D. Sands, C. C. Chang and D. L. Hart, *Appl. Phys. Lett.*, *58* (1991) 1557.
8 J. J. Kingston, F. C. Wellstood, P. Lerch, A. H. Miklich and J. Clarke, *Appl. Phys. Lett.*, *56* (1990) 189.
9 C. L. Jia, B. Kabius, K. Urban, K. Herrman, G. J. Cui, J. S. Schubert, W. Zandler, A. I. Braginski and C. Heiden, *Physica C*, *171* (1991) 545.
10 J. J. Kingston, F. C. Wellstood, D. Quan, and J. Clarke, *IEEE Trans. Magn.*, *27* (1991) 974.
11 F. K. Shokoohi, L. M. Schiavone, C. T. Rogers, A. Inam, X. D. Wu, L. Nazar and T. Venkatesan, *Appl. Phys. Lett.*, *55* (1989) 2661.